Atmos. Chem. Phys. Discuss., 13, 21507–21540, 2013
www.atmos-chem-phys-discuss.net/13/21507/2013/
doi:10.5194/acpd-13-21507-2013

Atmospheric Chemistry and Physics
Discussions
Open Access

Source, transport and impacts of a heavy dust event in the Yangtze River Delta, China in 2011

X. Fu[1], S. X. Wang[1,2], Z. Cheng[1], J. Xing[1,3], B. Zhao[1], J. D. Wang[1], and J. M. Hao[1,2]

[1]State Key Joint Laboratory of Environment Simulation and Pollution Control, School of Environment, Tsinghua University, Beijing 100084, China
[2]State Environmental Protection Key Laboratory of Sources and Control of Air Pollution Complex, Beijing 100084, China
[3]US Environmental Protection Agency, Research Triangle Park, NC, USA

Received: 8 June 2013 – Accepted: 5 August 2013 – Published: 20 August 2013

Correspondence to: S. X. Wang (shxwang@tsinghua.edu.cn)

Published by Copernicus Publications on behalf of the European Geosciences Union.

Abstract

During 1 to 6 May 2011, a dust event was observed in the Yangtze River Delta region (YRD). The highest PM_{10} concentration reached over 1000 µg m^{-3} and the visibility was below 3 km. In this study, the Community Multi-scale Air Quality modeling system (CMAQ5.0) coupled with an in-line windblown dust model was used to simulate the formation, spatial and temporal characteristics of this dust event, and analyze its impacts on deposition and photochemistry. The threshold friction velocity for loose smooth surface in the dust model was revised based on Chinese data to improve the model performance. The comparison between predictions and observations indicates the revised model can reproduce the transport and pollution of the event. The simulation results show that the dust event was affected by formation and transport of Mongolian cyclone and cold air. Totally about 695 kt dust particles (PM_{10}) were emitted in Xinjiang Province and Mongolia during 28 to 30 April, the dust band swept northern, eastern China and then arrived in the YRD region on 1 May 2011. The transported dust particles increased the mean surface layer concentrations of PM_{10} in the YRD region by 372 % during 1 to 6 May and the impacts weakened from north to south due to the removal of dust particles along the path. Accompanied by high PM concentration, the dry deposition, wet deposition and total deposition of PM_{10} in the YRD reached 184.7 kt, 172.6 kt and 357.32 kt, respectively. These deposited particles are very harmful because of their impacts on urban environment as well as air quality and human health when resuspending in the atmosphere. Due to the impacts of mineral dust on atmospheric photolysis, the concentrations of O_3 and OH were reduced by 1.5 % and 3.1 % in the whole China, and by 9.4 % and 12.1 % in the YRD region, respectively. The work of this manuscript is meaningful for understanding the dust emissions in China as well as for the application of CMAQ in Asia. It is also helpful to understand the formation mechanism and impacts of dust pollution in the YRD.

1 Introduction

Mineral dust is the largest single contributor to particulate matter in the atmosphere (Forster et al., 2007; Rind et al., 2009). China is one of regions which are usually affected by dust storms, especially in spring. The dust particles mainly originate from deserts in northern China and Mongolia (Zhang et al., 2003), which can reach Taiwan, southern China, Korea and even North America (Ault et al., 2011; Fan et al., 2013; Lin et al., 2012; Park et al., 2013). Suspended dust particles can be transported a long distance as carriers and reaction sites of many harmful species, such as fungal spores, microorganisms and anthropogenic pollutants including NO_X, VOC, and Pb (Huang et al., 2010; Lee et al., 2009). Some studies showed that the number of people with lung inflammation or stroke increased significantly during dust storm episode (Ichinose et al., 2008; Kang et al., 2013). It can also impact the radiation directly by absorption and scattering (Sokolik et al., 2001; Sun et al., 2012), and indirectly serve as cloud condensation nuclei (CCN) (Smoydzin et al., 2012; Solomos et al., 2012). Finally, dust particles can be removed by dry and wet depositions, which can take new nutrients into the surface water and may also result in acidification (Doney et al., 2007; Shi et al., 2012).

Numerical modeling is a useful method to analyze the characteristics of a dust event. In the recent decade, numerous physical or empirical based numerical models have been developed to describe the formation and transport of dust particles (e.g. Han et al., 2004; Wang et al., 2012a; Zender et al., 2003). They are usually implemented into air quality or climate models and used to analyze the impacts of dust particles on air quality, biogeochemical cycling, climate, and so on (Han et al., 2012; Wang et al., 2010a; Yan et al., 2012).The Community Multiscale Air Quality modeling system (CMAQ) developed by the United States Environmental Protection Agency (US EPA) is one of the widely-used air quality models (Knipping et al., 2006; Wang et al., 2010c; Wang et al., 2012b). Wang et al. (2012a) implemented an online dust emission and heterogeneous chemistry module into CMAQ version 4.7. Tong et al. (2012) developed

ACPD
13, 21507–21540, 2013

a dust emission model called FENGSHA and used it to estimate the dust emission in the United States. Based on Tong's work, the dust model was coupled with the newest version of CMAQ (CMAQ5.0) and was officially released in February 2012 (http://www.cmaq-model.org/). Up to now, this model has been used in the US only and the performance in other regions, especially in East Asia, still need to be evaluated.

The Yangtze River Delta (YRD), located in the eastern part of China, is one of China's most developed and densely populated regions. This region covers 213 340 km^2, only about 2.22 % of China's territory. However, A few metropolitan cities such as Shanghai, Nanjing, Suzhou, and Hangzhou locate in the YRD. Therefore, it lives 11.65 % of the national population, produces 21.51 % of the GDP, consumes 16.57 % of the national energy and bears 16.26 % of the total vehicle population in 2010 (National Bureau of Statistics of China, 2011a, b). Previous observations have indicated the long range transport of dust particles may significantly contribute to the particulate pollution in Shanghai, the largest mega-city in this area (Huang et al., 2010; Fu et al., 2010). Therefore, it is necessary to quantify the impacts of dust transport on regional air quality in the YRD region.

In this paper, we analyzed a strong dust event observed in the YRD region during 1 to 6 May 2011 using the CMAQ5.0 with a new in-line windblown dust model. In Sect. 2, a detailed description of model system is presented. Section 3 analyzes the dust emission characteristics in this event. Section 4 evaluates the model performance on meteorological conditions and pollutants concentration predictions. A further analysis of this dust event, including meteorological conditions, dust transport, effects of dust on deposition and photochemistry is also presented. Major findings and conclusions are summarized in Sect. 5.

ACPD
13, 21507–21540, 2013

2 Model description

2.1 Simulation domain and episode

One-way triple nesting simulation domains are used in this study, as shown in Fig. 1. They are based on the Lambert projection with the two true latitudes of 25° N and 40° N. Domain 1 covers most of China with a grid resolution of 36 km × 36 km; Domain 2 covers the eastern China with a grid resolution of 12 km × 12 km; Domain 3 covers the Yangtze River Delta region with a grid resolution of 4 km × 4 km. From 1 May 2011, an obvious increase of the PM concentration in the YRD region was observed and the $PM_{2.5}/PM_{10}$ ratio was only 25 %, which may be affected by dust storm. Considering the transport of dust, the simulation episode chosen is from 28 April to 6 May 2011.

2.2 CMAQ model configurations and inputs

The Community Multi-scale Air Quality modeling system version 5. (CMAQ5.0) with the updated 2005 Carbon Bond gas-phase mechanism (CB05) and the AERO6 aerosol module was applied in this study, which was officially released in February 2012. CB05 is enhanced by using the updated toluene chemistry (Whitten et al., 2010), modifying rate constants for N_2O_5 hydrolysis and adding reactions of xylene and toluene with chlorine radical. For aerosol module, AERO6 reflects many new features and improvements over AERO5. The enhancements include splitting primary $PM_{2.5}$ emissions into 18 species; incorporation of ISORROPIAv2.1 (Fountoukis and Nenes, 2007); update of POA aging (Simon and Bhave, 2012); addition of a new in-line windblown dust model (Tong et al., 2012); update of SOA yield parameterization. The vertical resolution in this study is 23 layers and the corresponding sigma levels are 1.000, 0.995, 0.988, 0.980, 0.970, 0.956, 0.938, 0.916, 0.893, 0.868, 0.839, 0.808, 0.777, 0.744, 0.702, 0.648, 0.582, 0.500, 0.400, 0.300, 0.200, 0.120, 0.052, and 0.000.

The Weather Research & Forecasting Model (WRF) version 3.3.1 was used to generate the meteorological fields. The first guess fields were obtained from final operational

Discussion Paper | Discussion Paper | Discussion Paper | Discussion Paper |
ACPD
13, 21507–21540, 2013
Sources and impacts of a dust event in the YRD
X. Fu et al.

global analysis data of the National Center for Environmental Prediction (NCEP). The Automated Data Processing (ADP) data was used to the analysis of four-dimensional data assimilation (FDDA). The physical options used in the WRF model were Morrison double-moment microphysics scheme (Morrison et al., 2009), the Rapid Radiative Transfer Model for GCMs (RRTMG) shortwave and longwave radiation scheme (Mlawer and Clough., 1998; Mlawer et al., 1997), Pleim–Xiu land surface scheme (Xiu and Pleim, 2001), ACM2 PBL scheme (Pleim, 2007), and Kain-Fritsch cumulus scheme (Kain, 2004).

In this study, the anthropogenic emission inventory was developed based on the information provided by Fu et al. (2013), Zhao et al. (2013), and the Trace-P emissions (Streets et al., 2003). For the YRD region (including Jiangsu, Zhejiang and Shanghai), the data were mainly from Fu et al. (2013), which is with higher spatial resolution than the emission in Zhao et al. and TRACE-P. For other provinces in China except for the YRD, the data were from Zhao et al. (2013). For other Asian countries, TRACE-P dataset was used. The biogenic emissions were calculated by MEGAN (Guenther et al., 2006). The total emissions for major pollutants (not including dust emissions) are listed in Table 1.

In order to evaluate the performance of the dust model and the impacts of dust emissions, three simulations are conducted in this study, including DUST_DEFAULT, DUST_REVISED and DUST_OFF. As shown in Table 2, here DUST_DEFAULT means the situation that the dust model with officially-released parameters is used. It is designed to evaluate the performance of the default dust model for this dust event. For DUST_REVISED, parameters including the threshold friction velocity for loose smooth surface and $PM_{2.5}/PM_{10}$ ratio are chosen based on Chinese data. In order to analyze the impacts of dust, another simulation (DUST_OFF) is also conducted, which refers to the situation that the dust model is turned off.

ACPD
13, 21507–21540, 2013

2.3 The in-line windblown dust model in CMAQ5

The dust emissions were generated by the new in-line windblown dust model in CMAQ5.0 (Tong et al., 2012). The vertical flux F ($\mathrm{g\,m^{-2}\,s^{-1}}$) was calculated by the following formula:

$$F = \sum_{i,j} K \cdot A \cdot \frac{\rho}{g} \cdot S_i \cdot \mathrm{SEP} \cdot u_* \cdot (u_*^2 - u_{*ti,j}^2) \text{ for } u_* > u_{*t} \tag{1}$$

Where i is the type of erodible lands, including shrub land, shrub grass and barren land; j is the soil types. Different soil types have different fractions of clay, silt and sand; K represents the ratio of vertical flux to horizontal sediment flux, which is associated with the clay content (%) and calculated by the following formula (Marticorena and Bergametti, 1995; Tong et al., 2012):

$$K = \begin{cases} 10^{0.134[\text{clay\%}]-6} & \text{for} \quad \text{clay\%} < 20\,\% \\ 0.0002 & \text{for} \quad \text{clay\%} \geq 20\,\% \end{cases} \tag{2}$$

A is the particle supply limitation; ρ is the air density; g is gravitational constant; S ($\mathrm{m^2}$) is the area of dust source, which is based on the MODIS land use data. For the three erodible land types, it assumes that the fraction of erodible lands capable of emitting dust is 0.5, 0.25 and 0.75, respectively; SEP is the soil erodibility factor, which is determined by the following formula:

$$\mathrm{SEP} = 0.08 \cdot \text{clay\%} + 1.00 \cdot \text{silt\%} + 0.12 \cdot \text{sand\%} \tag{3}$$

u_* ($\mathrm{m\,s^{-1}}$) is the friction velocity, which directly comes from the output of WRF.

In this equation, u_{*t} is the threshold friction velocity, which controls the intensity and the onset of dust emissions. It is expressed by $u_{*ti,j} = u'_{*ti,j} \cdot f_{di,j} \cdot f_{mi,j}$, considering the effects of surface roughness ($f_{di,j}$), soil moisture and snow cover ($f_{mi,j}$). $u'_{*ti,j}$ is

ACPD
13, 21507–21540, 2013

the threshold friction velocity for loose smooth surface. The default value of $u'_{*ti,j}$ is based on American data and set as 0.7 averagely, which is used in the simulation of DUST_DEFAULT. For the simulation DUST_REVISED, it was chosen as 0.3 based on Chinese local measurements (Li et al., 2007). Besides, different from the default value, the $PM_{2.5}/PM_{10}$ ratio for dust emission was chosen as 0.1 (Niu et al., 2003; Wang et al., 2012a). For other parameters, the default values in the model were used.

3 Dust emissions

The simulation results of DUST_REVISED indicated that about 695 kt dust particles (PM_{10}) were emitted in Xinjiang and Mongolia during 28 to 30 April 2011. Figures 2 and 3 show the spatio-temporal characteristic of dust emissions. On 28 April, a large amount of dust particles (about 145 kt) were generated up in Xinjiang Province and southwestern Mongolia by the strong northwestern wind. On 29 April, more new dust particles (about 515 kt) were emitted in south Mongolia and the highest density of dust emission could reach above 7 t km^{-2}. The largest value of total dust emission for the whole region occurred at 1500 BJT on 29 April, about 66.8 kt h^{-1}. Another small amount of dust particles were emitted on 30 April, only about 35 kt. As shown in Fig. 3, the predicted total dust emissions based on DUST_DEFAULT were only about 11 kt and underestimated by 98 % compared with that of DUST_REVISED. The default threshold friction velocity for loose smooth surface (about 0.7) was too high for Asian dust sources.

4 Results and discussion

4.1 Evaluation of meteorological simulations

The accuracy of the meteorological prediction is the foundation of air quality simulation. Table 3 summarizes the statistical performance of 10 m wind speed and wind direction

ACPD
13, 21507–21540, 2013

(WS10 and WD10, respectively), 2 m temperature (T2) and 2 m humidity (H2). Hourly or every third hour observation data were obtained from the National Climatic Data Center (NCDC) for 1955 stations within Domain 1, 787 stations within Domain2 and 90 stations within Domain 3. The statistical parameters contain mean observation (Mean OBS), mean simulation (Mean SIM), bias, gross error (GE), root mean square error (RMSE), and the index of agreement (IOA), which are explained in details in Baker (2004). The benchmark values are suggested by Emery et al. (2001), which are based on results of many studies in US. These values are also used as reference standards in this study.

As shown in Table 3, the performance of WS10 is satisfactory. The bias, GEs, RMSEs and IOA values of all the three domains are within the benchmark range. For WD10, while the biases are below the 10°, the gross errors are 2 to 21° higher than the benchmark value. The high gross errors may result from a caveat in treating the wind direction vector as a scalar in the calculation method, as described in previous studies (Wang et al., 2010b; Zhang et al., 2006). The T2 predictions were slightly underestimated. But the IOA values for all three domains are close to one, indicating an acceptable performance. The results for Domain 1 (36 km grid) are relatively worse, which mainly result from the poor representation of steep terrains with a coarse grid resolution (Wang et al., 2012a). For humidity, generally the model can reproduce the observed values. For Domain 2 (12 km grid) and Domain 3 (4 km grid), all statistical parameters are within the benchmark range. For Domain 1 (36 km grid), the bias and GE values is above the benchmark, but the IOA value is a little lower. Because the benchmark values are mostly based on the domains with 4 km or 12 km resolution and the meteorological predictions can be more accurate than that for 36 km, this slight underestimation is acceptable.

4.2 Evaluation of pollutants concentration predictions

Two observational datasets were used for model evaluation. The first one is the hourly PM_{10} concentration for official monitoring sites in Mainland China obtained from the

ACPD
13, 21507–21540, 2013

Ministry Environmental Protection of the People's Republic of China (MEP) (http://113.108.142.147:20035/emcpublish/). Considering that the data of some monitoring sites are missing during this simulation episode, 546 monitoring sites (as shown in Fig. 1) were chosen for the model evaluation. Another dataset was from the field measurement by Tsinghua University for 3 monitoring sites in the YRD region (as shown in Fig. 4), including Shanghai city, Nanjing in Jiangsu Province and Ningbo in Zhejiang Province.

Table 4 shows the hourly PM_{10} concentrations from observations and simulations DUST_OFF, DUST_DEFAULT and DUST_REVISED for all 3 domains. The results of DUST_OFF underestimate the PM_{10} concentration significantly, with NMBs of −47.1 %, −37.8 % and −72.2 % for the Domain 1, 2, and 3, respectively. Compared with the results of DUST_OFF, the model performance of DUST_DEFAULT was not improved substantially. The poor results may result from the significant underestimation of dust emissions by the dust model with default parameters, as described in Sects. 2 and 3. The model performance of DUST_REVISED is significantly improved compared with that of DUST_DEFAULT. The NMBs for Domain 1, 2, and 3 are −10.9 %, 7.1 % and −13.6 %, respectively. The correlation coefficients (R) are at the range of 0.4–0.6.

In order to evaluate the performance of DUST_REVISED further, we compared the temporal variations of simulated hourly PM_{10} and $PM_{2.5}$ concentration with observations in 3 monitoring sites in the YRD region (as shown in Fig. 4). From 1 to 4 May, a strong dust event occurred in this region and the highest PM_{10} concentration could reach more than 1000 $\mu g\,m^{-3}$. In general, the model could reproduce the temporal trends and high PM_{10} concentrations well. The NMBs of PM_{10} predictions for Nanjing, Shanghai and Ningbo are −17 %, −35 % and 4 %, respectively, and the correlation coefficients (R) are about 0.65–0.85. Relative large deviations occur at a few moments (e.g. early of 2 May in Nanjing, early of 3 May in Shanghai and middle of 2 May in Ningbo), which may result from the poor prediction of wind speed or wind direction at these moments. For example, at early time of 3 May in Shanghai, the simulated wind direction is 20–40°, but the observed wind direction is 90–180°. On 3 May, dust particles were transported from sea to land and therefore this deviation of wind direction may lead to the underestimation of PM in Shanghai. For the $PM_{2.5}$ concentration, the model could reproduce its variation trend well and the correlation coefficients (*R*) are about 0.6–0.8. However, the model tends to overestimate the $PM_{2.5}$ concentration slightly, with NMBs of 14 %, 28 % and 41 % for Nanjing, Shanghai and Ningbo, respectively. This overestimation may be affected by the splitting between $PM_{2.5}$ and $PM_{2.5-10}$, because we just simply allocate 10 % of dust PM_{10} emission to $PM_{2.5}$. Anyway, the comparison results demonstrate the CMAQ5.0 with the revised dust module could capture the PM variation reasonably well.

4.3 Analysis of metrological condition for this dust event

As shown in Fig. 5, on 28 April, a cyclone was formed in the Mongolia, associating with a cold front in the rear part of the low-pressure system. Strong surface winds (8–14 $m\,s^{-1}$) occurred in eastern Xinjiang and western Mongolia, generating a dust storm there. The Mongolian cyclone and air mass developed further, generating a stronger dust storm in middle-southern Mongolia on 29 April. These possible locations of dust storms are in accordance with the modeling results (Fig. 2). Then these two dust bands mixed together and moved to eastern and southern direction. On 1 May, the observed concentration of PM_{10} in the YRD began to increase (Fig. 4), when the high pressure associated with cold air arrived in this region. As shown in Fig. 6, the pressure and wind speed began to increase, and the temperature began to decrease. In Shanghai, the pressure increased from 1003.5 mb on 1 May to 1016 mb on 3 May, and the temperature decreased by 5–10 °C. Controlled by high pressure, the wind became relatively light from the midday of 3 May, which is adverse to the dispersion of dust particles. Until the end of 4 May, the temperature and wind speed began to increase, the pressure began to decrease and then this dust event ended.

4.4 Dust transport and its impacts on PM_{10} concentration

Figure 7 shows the spatio-temporal variation of PM_{10} concentration differences between DUST_REVISED and DUST_OFF, which helps to understand the transport of this dust event and the impacts of dust storm on PM_{10} concentration. The emitted dust particles mixed together and moved on toward eastern and southern direction. The PM_{10} concentration at the sites near the dust sources, i.e. Lanzhou city in Gansu Province, could reach nearly 5000 $\mu g\,m^{-3}$. On 30 April, the dust began to affect the eastern and central China. For example, the PM_{10} concentration in Tianjin city increased from 50 $\mu g\,m^{-3}$ to 1100 $\mu g\,m^{-3}$. The dust band arrived in the YRD on 1 May and the PM_{10} concentration in Shanghai increased from 50 $\mu g\,m^{-3}$ to 640 $\mu g\,m^{-3}$ (as shown in Fig. 4). The maximum PM_{10} value reached 1000 $\mu g\,m^{-3}$ on 2 May. Another part of the dust band also reached Korea and even Japan, but was blew back to the YRD by the southwestern wind on 3 May. From 4 May, the impact of dust on the YRD region began to decline. By comparing the simulation results of DUST_REVISED and DUST_OFF, the dust emissions increased the mean surface layer concentrations of PM_{10} in the YRD region by 372 % during 1 to 6 May and the impacts weakened from north to south due to the deposition of dust particles along the path.

4.5 Deposition of dust aerosols in the YRD region

Dust particles can be finally removed by dry and wet depositions. During 1 to 6 May, the dry deposition, wet deposition and total deposition of PM_{10} are 184.7 kt, 172.6 kt and 357.32 kt, respectively, of which $PM_{2.5}$ depositions account for 5.7 %, 36.4 % and 20.5 %, respectively. Fig. 8 shows the spatial distribution of dry deposition (DDEP), wet deposition (WDEP), total deposition (TDEP) and the difference of total deposition between DUST_REVISED and DUST_OFF situation (TDEP_DIFF) for PM_{10} in the Domain 3 (covering the YRD region) in these six days.

The dry depositions of PM_{10} account for 51.7 % of the total. In general, the dry depositions in Jiangsu Province and Shanghai city were larger than that in Zhejiang

Province, which was affected by the PM_{10} concentration. Dust particles were transported from north to south and the concentration became lower at the end of the transport path. Meanwhile, relatively high values can also be seen at some urban or forest regions. Except for the impacts of PM_{10} concentration, the larger associated parameters (e.g. the surface roughness length and leaf-area index) can lead to higher deposition velocity (Kumar et al., 2008; Fan et al., 2009). Wet depositions are associated with precipitation and dust concentration. As shown in Fig. 8, wet depositions mainly occur in East Sea, Shanghai, southern Zhejiang etc. Comparison between the results of DUST_REVISED and DUST_OFF shows that the long range transport of dust particles increased the total deposition of PM_{10} in the YRD by 1082 %, of which dry deposition increased by 2398 % and wet deposition increased by 655 %. These deposited particles are very harmful because of their impacts on urban environment as well as on air quality and human health when resuspending in the atmosphere.

4.6 Impacts of dust storm on photochemistry

Dust particles have important effects on photolysis rates of chemical oxidants through their effects on solar radiation by absorption and scattering (Bian and Zender, 2003; Ying et al., 2011). An online photolysis module has been incorporated in CMAQ 5., which allows the calculation of actinic fluxes and photolysis rates for every grid at each time step based on the changes in particle concentrations. The detail description is given by Binkowski et al. (2007). Here, we don't consider the effects though the feedbacks on meteorology, such as temperature and pressure.

The impacts of dust on photolysis chemistry through their effects on the actinic flux are analyzed by comparing the results of DUST_REVISED with that of DUST_OFF. During 28 April to 6 May, the photolysis rate coefficient (*J* values) for NO_2 was reduced by about 24 % averagely in whole Domain 1. As shown in Fig. 9a, the perturbations are mainly in dust source regions and along the dust transport path. The variation of photolysis rates has important impacts on the concentrations of O_3 and OH. Due to the dust storm, the surface O_3 concentrations reduced about 1.5 % averagely for Domain

1 and the maximum reached 6 ppbv. Figure 9b shows that the largest perturbations of O_3 occurred in a region including China Sea, eastern China and Korea. One major reason is that air mass with dust stayed in this region for two days (2–3 May, as shown in Fig. 7) due to the high pressure control. The decrease of OH was about 3.1 % averagely in whole Domain 1, resulting from the reductions in O(1D) generated by ultraviolet photolysis of O_3 (Bian and Zender, 2003). As shown in Fig. 9c, the reduction of OH concentrations is well correlated with the spatial distribution of JNO_2 reduction, due to the short chemical lifetime of OH. For the YRD region, because of the reduction of local generation and long transport, the O_3 and OH concentrations were decreased by 9.4 % and 12.1 % averagely.

5 Conclusions

Dust storm, which happens several times each year, has significant impacts on the air quality not only in the northern Chinese cities but also in the YRD in spring. A strong dust event was observed in the Yangtze River Delta region during 1 to 6 May 2011, when the PM_{10} concentration could reach 1000 $\mu g\,m^{-3}$. In this study, the CMAQ5.0 coupled with a new in-line windblown dust model was used to analyze the event and the threshold friction velocity for loose smooth surface in the dust model was revised according to Chinese data. The predictions of the model DUST-REVISED agreed well with the observations and were greatly improved compared with DUST-DEFAULT.

The total dust emissions for this event were estimated to be 695 kt, mainly emitted in Xinjiang and Mongolia during 28 to 30 April 2011. The metrology analysis indicates that this dust storm was mainly affected by Mongolian cyclone and cold air. The dust particles moved toward eastern and southern direction by the wind and affected most part of China. On 1 May, the dust band arrived in the YRD, which increased the PM_{10} concentration and decreased the visibility significantly. The impact of dust on the YRD region began to decrease from 4 May. The transported dust particles increased the mean surface layer concentrations of PM_{10} in the YRD region by 372 % during 1 to 6

May and the impacts weakened from north to south due to the removal of dust particles along the path.

A large amount of particles were deposited in the YRD region, which were very harmful to urban environment and public health. During 1 to 6 May, the dry deposition, wet deposition and total deposition of PM_{10} were 184.7 kt, 172.6 kt and 357.32 kt, respectively. In the YRD, the dust storm tends to increase the total PM_{10} deposition by 1082 %, dry deposition by 2398 % and wet deposition by 655 %.

The dust particles have significant impacts on photolysis rates of chemical oxidants through their effects on solar radiation by absorption and scattering. The comparison between DUST_REVISED and DUST_OFF showed that the photolysis rate coefficient (J values) for NO_2 was reduced by about 24 % averagely in whole Domain 1. The perturbations of O_3 and OH were −1.5 % and −3.1 % averagely in whole Domain 1. For the YRD region, because of the reduction of local generation and reduction of long range transport, the O_3 and OH concentrations are decreased by 9.4 % and 12.1 %. The photolysis rates can be also affected by temperature and pressure, but here we don't consider the effects though the feedbacks on meteorology. It's better and meaningful to consider this effect by running the online WRF-CMAQ system in the future.

CMAQ is a wide-used air quality model and the implementation of the new dust emission model is a very meaningful work for CMAQ development. Meanwhile, more work need to do for better model performance. For example, the current CMAQ version does not consider about some important heterogeneous reactions on the surface of dust particles, such as SO_2, O_3, and H_2O_2, which might be an important contributor to the impacts of dust on pollutant concentration (Bian and Zender, 2003; Zhu et al., 2010). Therefore more heterogeneous reactions shall be coupled into the model in future.

Acknowledgements. This work was sponsored by National Natural Science Foundation of China (21221004), Strategic Priority Research Program of the Chinese Academy of Sciences (XBD05020300), and the MEP's Special Funds for Research on Public Welfares (No. 201009001). The corresponding author, Shuxiao Wang, is supported by the Program for New

Century Excellent Talents in University (NCET-10-0532). The authors also appreciate it very much for the help on CMAQ5.0 from David Wong at US Environmental Protection Agency.

References

Ault, A. P., Williams, C. R., White, A. B., Neiman, P. J., Creamean, J. M., Gaston, C. J., Ralph, F. M., and Prather, K. A.: Detection of Asian dust in California orographic precipitation, J. Geophys. Res.-Atmos., 116, D16205, doi:10.1029/2010jd015351, 2011.

Baker, K.: Meteorological Modeling Protocol for Application to $PM_{2.5}$/haze/ozone Modeling Projects, Lake Michigan Air Directors Consortium/Midwest Region Planning Organization, Des Plaines, Illinois, 2004.

Bian, H. S. and Zender, C. S.: Mineral dust and global tropospheric chemistry: relative roles of photolysis and heterogeneous uptake, J. Geophys. Res.-Atmos., 108, 4672, doi:10.1029/2002jd003143, 2003.

Binkowski, F. S., Arunachalam, S., Adelman, Z., and Pinto, J. P.: Examining photolysis rates with a prototype online photolysis module in CMAQ, J. Appl. Meteorol. Clim., 46, 1252–1256, doi:10.1175/jam2531.1, 2007.

Doney, S. C., Mahowald, N., Lima, I., Feely, R. A., Mackenzie, F. T., Lamarque, J.-F., and Rasch, P. J.: Impact of anthropogenic atmospheric nitrogen and sulfur deposition on ocean acidification and the inorganic carbon system, P. Natl. Acad. Sci. USA, 104, 14580–14585, doi:10.1073/pnas.0702218104, 2007.

Emery, C., Tai, E., and Yarwood, G.: Enhanced meteorological modeling and performance evaluation for two texas episodes, Report to the Texas Natural Resources Conservation Commission, ENVIRON, International Corp, Novato, CA, 2001.

Evans, B. T. N. and Fournier, G. R.: Simple approximation to extinction efficiency valid over all size parameters, Appl. Optics, 29, 4666–4670, 1990.

Fan, J.-L., Hu, Z. Y., Wang, T. J., and Zhou, J.: Dynamics of dry deposition velocities of atmospheric nitrogen compounds in a broadleaf forestland, China Environmental Science, 29, 574–577, 2009.

Fan, Q., Shen, C., Wang, X. M., Li, Y., Huang, W., Liang, G. X., Wang, S. Y., and Huang, Z. E.: Impact of a dust storm on characteristics of particle matter (PM) in Guangzhou, China, Asia-Pac. J. Atmos. Sci., 49, 121–131, doi:10.1007/s13143-013-0013-2, 2013.

ACPD

13, 21507–21540, 2013

Forster, P., Ramaswamy, V., Artaxo, P., Berntsen, T., Betts, R., Fahey, D. W., Haywood, J., Lean, J., Lowe, D. C., Myhre, G., Nganga, J., Prinn, R., Raga, G., Schultz, M., and Van Dorland, R.: Changes in atmospheric constituents and in radiative forcing, in: Climate Change 2007: The Physical Science Basis, Contribution of Working Group I to the Fourth Assessment Report of the Intergovernmental Panel on Climate Change, edited by: Solomon, S., Qin, D., Manning, M., Chen, Z., Marquis, M., Avert, K. B.,Tignor, M., and Miller, H. L., Cambridge University Press, Cambridge, UK, New York, NY, USA, 2007.

Fountoukis, C. and Nenes, A.: ISORROPIA II: a computationally efficient thermodynamic equilibrium model for $K+-Ca2+-Mg2+-NH_4+-Na+-SO_42--NO_3--Cl--H_2O$ aerosols, Atmos. Chem. Phys., 7, 4639–4659, doi:10.5194/acp-7-4639-2007, 2007.

Fu, Q., Zhuang, G., Li, J., Huang, K., Wang, Q., Zhang, R., Fu, J., Lu, T., Chen, M., Wang, Q., Chen, Y., Xu, C., and Hou, B.: Source, long-range transport, and characteristics of a heavy dust pollution event in Shanghai, J. Geophys. Res.-Atmos., 115, D00k29, doi:10.1029/2009jd013208, 2010.

Fu, X., Wang, S. X., Zhao, B., Xing, J., Cheng, Z., Liu, H., and Hao, J. M.: Emission inventory of primary pollutants and chemical speciation in 2010 for the Yangtze River Delta region, China, Atmos. Environ., 70, 39–50, doi:10.1016/j.atmosenv.2012.12.034, 2013.

Guenther, A., Karl, T., Harley, P., Wiedinmyer, C., Palmer, P. I., and Geron, C.: Estimates of global terrestrial isoprene emissions using MEGAN (Model of Emissions of Gases and Aerosols from Nature), Atmos. Chem. Phys., 6, 3181–3210, doi:10.5194/acp-6-3181-2006, 2006.

Han, X., Ge, C., Tao, J. H., Zhang, M. G., and Zhang, R. J.: Air quality modeling for a strong dust event in East Asia in March 2010, Aerosol Air Qual. Res., 12, 615–628, doi:10.4209/aaqr.2011.11.0191, 2012.

Han, Z. W., Ueda, H., Matsuda, K., Zhang, R. J., Arao, K., Kanai, Y., and Hasome, H.: Model study on particle size segregation and deposition during Asian dust events in March 2002, J. Geophys. Res.-Atmos., 109, D19205, doi:10.1029/2004jd004920, 2004.

Huang, K., Zhuang, G., Li, J., Wang, Q., Sun, Y., Lin, Y., and Fu, J. S.: Mixing of Asian dust with pollution aerosol and the transformation of aerosol components during the dust storm over China in spring 2007, J. Geophys. Res.-Atmos., 115, D00k13, doi:10.1029/2009jd013145, 2010.

Ichinose, T., Yoshida, S., Hiyoshi, K., Sadakane, K., Takano, H., Nishikawa, M., Mori, I., Yanagisawa, R., Kawazato, H., Yasuda, A., and Shibamoto, T.: The effects of microbial materials

adhered to Asian sand dust on allergic lung inflammation, Arch. Environ. Con. Tox., 55, 348–357, doi:10.1007/s00244-007-9128-8, 2008.
Kain, J. S.: The Kain–Fritsch convective parameterization: an update, J. Appl. Meteorol., 43, 170–181, doi:10.1175/1520-0450(2004)043<0170:TKCPAU>2.0.CO;2, 2004.
Kang, J. H., Liu, T. C., Keller, J., and Lin, H. C.: Asian dust storm events are associated with an acute increase in stroke hospitalisation, J. Epidemiol. Commun. H., 67, 125–131, doi:10.1136/jech-2011-200794, 2013.
Knipping, E. M., Kumar, N., Pun, B. K., Seigneur, C., Wu, S. Y., and Schichtel, B. A.: Modeling regional haze during the BRAVO study using CMAQ-MADRID: 2. Source region attribution of particulate sulfate compounds, J. Geophys. Res.-Atmos., 111, D06303, doi:10.1029/2004jd005609, 2006.
Kumar, R., Srivastava, S. S., and Kumari, K. M.: Modeling dry deposition of S and N compounds to vegetation, Indian J. Radio Space, 37, 272–278, 2008.
Lee, S., Choi, B., Yi, S. M., and Ko, G.: Characterization of microbial community during Asian dust events in Korea, Sci. Total Environ., 407, 5308–5314, doi:10.1016/j.scitotenv.2009.06.052, 2009.
Li, W. Y., Shen, Z. B., Lu, S. H., and Li, Y. H.: Sensitivity tests of factors influencing wind erosion, Journal of Desert Research, 27, 984–993, 2007.
Lin, C. Y., Chou, C. C. K., Wang, Z. F., Lung, S. C., Lee, C. T., Yuan, C. S., Chen, W. N., Chang, S. Y., Hsu, S. C., Chen, W. C., and Liu, S. C.: Impact of different transport mechanisms of Asian dust and anthropogenic pollutants to Taiwan, Atmos. Environ., 60, 403–418, doi:10.1016/j.atmosenv.2012.06.049, 2012.
Mlawer, E. J. and Clough, S. A.: Shortwave clear-sky model-measurement intercomparison using RRTM, the 8th Atmospheric Radiation Measurement (ARM) Science Team Meeting, Tucson, Arizona, USA, 1998.
Mlawer, E. J., Taubman, S. J., Brown, P. D., Iacono, M. J., and Clough, S. A.: Radiative transfer for inhomogeneous atmospheres: RRTM, a validated correlated-*k* model for the longwave, J. Geophys. Res.-Atmos., 102, 16663–16682, doi:10.1029/97jd00237, 1997.
Morrison, H., Thompson, G., and Tatarskii, V.: Impact of cloud microphysics on the development of trailing stratiform precipitation in a simulated squall line: comparison of one- and two-moment schemes, Mon. Weather Rev., 137, 991–1007, doi:10.1175/2008mwr2556.1, 2009.
National Bureau of Statistics of China, China Statistical Yearbook 2011, China Statistics Press, Beijing, 2011a.

ACPD
13, 21507–21540, 2013

National Bureau of Statistics of China, China Energy Statistical Yearbook 2011, China Statistics Press, Beijing, 2011b.
Niu, S. J. and Sun, Z. B.: Aircraft observation of spatial and temporal characteristics of desert dust aerosol and $PM_{2.5}$, Annual Meeting of Chinese Meteorological Society, Beijing, 55-56-57-58, 2003.
Park, S. U., Choe, A., and Park, M. S.: A simulation of Asian dust events observed from 20 to 29 December 2009 in Korea by using ADAM2, Asia-Pac. J. Atmos. Sci., 49, 95–109, doi:10.1007/s13143-013-0011-4, 2013.
Pleim, J. E.: A combined local and nonlocal closure model for the atmospheric boundary layer. Part I: Model description and testing, J. Appl. Meteorol. Clim., 46, 1383–1395, doi:10.1175/jam2539.1, 2007.
Rind, D., Chin, M., Feingold, G., Streets, D., Kahn, R. A., Schwartz, S. E., and Yu, H.: Modeling the effects of aerosolson climate, in atmospheric aerosol properties and climate impacts, a Report by the US Climate Change Science Program and the Subcommittee on Global Change Research, edited by: Chin, M., Kahn, R. A., and Schwartz, S. E., National Aeronautics and Space Administration, Washington, DC, USA, 2009.
Shi, J. H., Gao, H. W., Zhang, J., Tan, S. C., Ren, J. L., Liu, C. G., Liu, Y., and Yao, X.: Examination of causative link between a spring bloom and dry/wet deposition of Asian dust in the Yellow Sea, China, J. Geophys. Res.-Atmos., 117, D17304, doi:10.1029/2012jd017983, 2012.
Simon, H. and Bhave, P. V.: Simulating the degree of oxidation in atmospheric organic particles, Environ. Sci. Technol., 46, 331–339, doi:10.1021/es202361w, 2012.
Smoydzin, L., Teller, A., Tost, H., Fnais, M., and Lelieveld, J.: Impact of mineral dust on cloud formation in a Saharan outflow region, Atmos. Chem. Phys., 12, 11383–11393, doi:10.5194/acp-12-11383-2012, 2012.
Sokolik, I. N., Winker, D. M., Bergametti, G., Gillette, D. A., Carmichael, G., Kaufman, Y. J., Gomes, L., Schuetz, L., and Penner, J. E.: Introduction to special section: outstanding problems in quantifying the radiative impacts of mineral dust, J. Geophys. Res.-Atmos., 106, 18015–18027, doi:10.1029/2000jd900498, 2001.
Solomos, S., Kushta, J., and Kallos, G.: Effects of airborne particles on cloud formation and precipitation: a modeling study, in: Air Pollution Modeling and Its Application XXI, edited by: Steyn, D. G. and Castelli, S. T., NATO Science for Peace and Security Series C-Environmental Security, 571–578, 2012.

Streets, D. G., Bond, T. C., Carmichael, G. R., Fernandes, S. D., Fu, Q., He, D., Klimont, Z., Nelson, S. M., Tsai, N. Y., Wang, M. Q., Woo, J. H., and Yarber, K. F.: An inventory of gaseous and primary aerosol emissions in Asia in the year 2000, J. Geophys. Res.-Atmos., 108, 8809, doi:10.1029/2002jd003093, 2003.

Sun, H., Pan, Z., and Liu, X.: Numerical simulation of spatial-temporal distribution of dust aerosol and its direct radiative effects on East Asian climate, J. Geophys. Res.-Atmos., 117, D13206, doi:10.1029/2011jd017219, 2012.

Tong, D., Dan, M., Lee, P., Saylor, R., Young, J., Simon, H., Bhave, P., Pouliot, G., and Mathur, R.: CMAQ modeling of natural and anthropogenic dust aerosols over the United States, 4th International Workshop on Air Quality Forecasting Research (IWAQFR), Geneva, Switzerland, 12–14 December 2012.

Wang, H., Zhang, X. Y., Gong, S. L., Chen, Y., Shi, G. Y., and Li, W.: Radiative feedback of dust aerosols on the East Asian dust storms, J. Geophys. Res.-Atmos., 115, D23214, doi:10.1029/2009jd013430, 2010a.

Wang, K., Zhang, Y., Nenes, A., and Fountoukis, C.: Implementation of dust emission and chemistry into the Community Multiscale Air Quality modeling system and initial application to an Asian dust storm episode, Atmos. Chem. Phys., 12, 10209–10237, doi:10.5194/acp-12-10209-2012, 2012a.

Wang, L. T., Jang, C., Zhang, Y., Wang, K., Zhang, Q., Streets, D., Fu, J., Lei, Y., Schreifels, J., He, K., Hao, J., Lam, Y.-F., Lin, J., Meskhidze, N., Voorhees, S., Evarts, D., and Phillips, S.: Assessment of air quality benefits from national air pollution control policies in China. Part I: Background, emission scenarios and evaluation of meteorological predictions, Atmos. Environ., 44, 3442–3448, doi:10.1016/j.atmosenv.2010.05.051, 2010b.

Wang, L. T., Xu, J., Yang, J., Zhao, X., Wei, W., Cheng, D., Pan, X., and Su, J.: Understanding haze pollution over the southern Hebei area of China using the CMAQ model, Atmos. Environ., 56, 69–79, doi:10.1016/j.atmosenv.2012.04.013, 2012b.

Wang, S. X., Zhao, M., Xing, J., Wu, Y., Zhou, Y., Lei, Y., He, K., Fu, L., and Hao, J.: Quantifying the air pollutants emission reduction during the 2008 Olympic Games in Beijing, Environ. Sci. Technol., 44, 2490–2496, doi:10.1021/es9028167, 2010c.

Whitten, G. Z., Heo, G., Kimura, Y., McDonald-Buller, E., Allen, D. T., Carter, W. P. L., and Yarwood, G.: A new condensed toluene mechanism for Carbon Bond CB05-TU, Atmos. Environ., 44, 5346–5355, doi:10.1016/j.atmosenv.2009.12.029, 2010.

Xiu, A. J. and Pleim, J. E.: Development of a land surface model, Part I: Application in a mesoscale meteorological model, J. Appl. Meteorol., 40, 192–209, doi:10.1175/1520-0450(2001)040<0192:DOALSM>2.0.CO;2, 2001.

Yan, H., Gao, H., Yao, X., and Wang, Z.: Simulating dry deposition fluxes of PM_{10} and particulate inorganic nitrogen over the eastern China seas during a severe Asian dust event using WRF-Chem model, Journal of Ocean University of China, 11, 301–314, doi:10.1007/s11802-012-1857-2, 2012.

Ying, Z., Tie, X., Madronich, S., Li, G., and Massie, S.: Simulation of regional dust and its effect on photochemistry in the Mexico City area during MILAGRO experiment, Atmos. Environ., 45, 2549–2558, doi:10.1016/j.atmosenv.2011.02.018, 2011.

Zender, C. S., Bian, H. S., and Newman, D.: Mineral Dust Entrainment and Deposition (DEAD) model: description and 1990s dust climatology, J. Geophys. Res.-Atmos., 108, 4416, doi:10.1029/2002jd002775, 2003.

Zhang, X. Y., Gong, S. L., Zhao, T. L., Arimoto, R., Wang, Y. Q., and Zhou, Z. J.: Sources of Asian dust and role of climate change versus desertification in Asian dust emission, Geophys. Res. Lett., 30, 2272, doi:10.1029/2003gl018206, 2003.

Zhang, Y., Liu, P., Pun, B., and Seigneur, C.: A comprehensive performance evaluation of MM5-CMAQ for the Summer 1999 Southern Oxidants Study episode – Part I: Evaluation protocols, databases, and meteorological predictions, Atmos. Environ., 40, 4825–4838, doi:10.1016/j.atmosenv.2005.12.043, 2006.

Zhao, B., Wang, S. X., Wang, J. D., Fu, J., Liu, T. H., Xu, J. Y., Fu, X., and Hao, J. M.: Impact of national NO_X and SO_2 emission control policies on particulate matter pollution in China, Atmos. Environ., 77, 453–463, 2013.

Zhu, S., Butler, T., Sander, R., Ma, J., and Lawrence, M. G.: Impact of dust on tropospheric chemistry over polluted regions: a case study of the Beijing megacity, Atmos. Chem. Phys., 10, 3855–3873, doi:10.5194/acp-10-3855-2010, 2010.

ACPD
13, 21507–21540, 2013

Table 1. The emissions of major pollutants for each domain during 28 April to 6 May.

	Unite	Domain 1	Domain 2	Domain 3
PM_{10}	10^3 t	543.6	329.7	28.5
$PM_{2.5}$	10^3 t	399.2	230.9	15.3
SO_2	10^3 t	706.6	501	36.5
NO_X	10^3 t	571.5	395.7	56.4
NH_3	10^3 t	432.7	276.1	30.1
VOC	10^9 mol	55	25.1	4

Table 2. Scenario design for model simulations.

Run Index	Model Configuration	Purpose
DUST_DEFAULT	The default parameters in the official version was used. (e.g.$u'_{*ti,j} \approx 0.7$ averagely and $PM_{2.5}/PM_{10} = 0.2$)	Performance evaluation of the default dust model
DUST_REVISED	The threshold friction velocity for loose smooth surface and $PM_{2.5}/PM_{10}$ ratio are chosen based on Chinese data ($u'_{*ti,j} \approx 0.3$ and $PM_{2.5}/PM_{10} = 0.1$)	Performance evaluation of the revised version
DUST_OFF	The dust model was turned off	Analysis of dust impacts

Table 3. Performance statistics of meteorological variables.

			Domain 1	Domain 2	Domain 3	Benchmark
Wind Speed (WS10)	Mean OBS	($m\,s^{-1}$)	3.53	3.26	3.50	
	Mean SIM	($m\,s^{-1}$)	3.48	3.23	3.29	
	Bias	($m\,s^{-1}$)	0.05	0.03	−0.21	$\leq \pm 0.5$
	GE	($m\,s^{-1}$)	1.35	1.21	0.99	≤ 2
	RMSE	($m\,s^{-1}$)	1.82	1.69	1.35	≤ 2
	IOA		0.82	0.80	0.83	≥ 0.6
Wind Direction (WD10)	Mean OBS	(°)	231	195	129	
	Mean SIM	(°)	220	200	128	
	Bias	(°)	2.5	3.4	1	$\leq \pm 10$
	GE	(°)	42	38	28	≤ 30
Temperature (T2)	Mean OBS	(K)	288.2	292.2	292.2	
	Mean SIM	(K)	286.3	291.4	290.8	
	Bias	(K)	−1.9	−0.8	−1.4	$\leq \pm 0.5$
	GE	(K)	2.9	2.	2.3	≤ 2
	RMSE	(K)	5.8	3.1	2.8	
	IOA		0.88	0.95	0.87	≥ 0.8
Humidity (H2)	Mean OBS	($g\,kg^{-1}$)	6.88	10.13	9.63	
	Mean SIM	($g\,kg^{-1}$)	6.95	10.12	9.11	
	Bias	($g\,kg^{-1}$)	0.07	−0.01	−0.52	$\leq \pm 1$
	GE	($g\,kg^{-1}$)	1.42	1.76	1.41	≤ 2
	RMSE	($g\,kg^{-1}$)	13.93	11.69	1.95	
	IOA		0.31	0.63	0.66	≥ 0.6

ACPD
13, 21507–21540, 2013

Table 4. Model performance for hourly PM_{10} concentrations.

		Domain 1	Domain 2	Domain 3
	Number of stations	546	405	82
	Mean Obs. ($\mu g\,m^{-3}$)	119	127	176
DUST_OFF	Mean Sim. ($\mu g\,m^{-3}$)	63	79	49
	Bias ($\mu g\,m^{-3}$)	−56	−48	−127
	NMB (%)	−47.1	−37.8	−72.2
	R	0.05	0.04	0.05
DUST_DEFAULT	Mean Sim. ($\mu g\,m^{-3}$)	64	81	51
	Bias ($\mu g\,m^{-3}$)	−55	−46	−125
	NMB (%)	−46.2	−36.2	−71
	R	0.07	0.06	0.13
DUST_REVISED	Mean Sim. ($\mu g\,m^{-3}$)	106	136	152
	Bias ($\mu g\,m^{-3}$)	−13	9	−24
	NMB (%)	−10.9	7.1	−13.6
	R	0.42	0.46	0.63

ACPD
13, 21507–21540, 2013

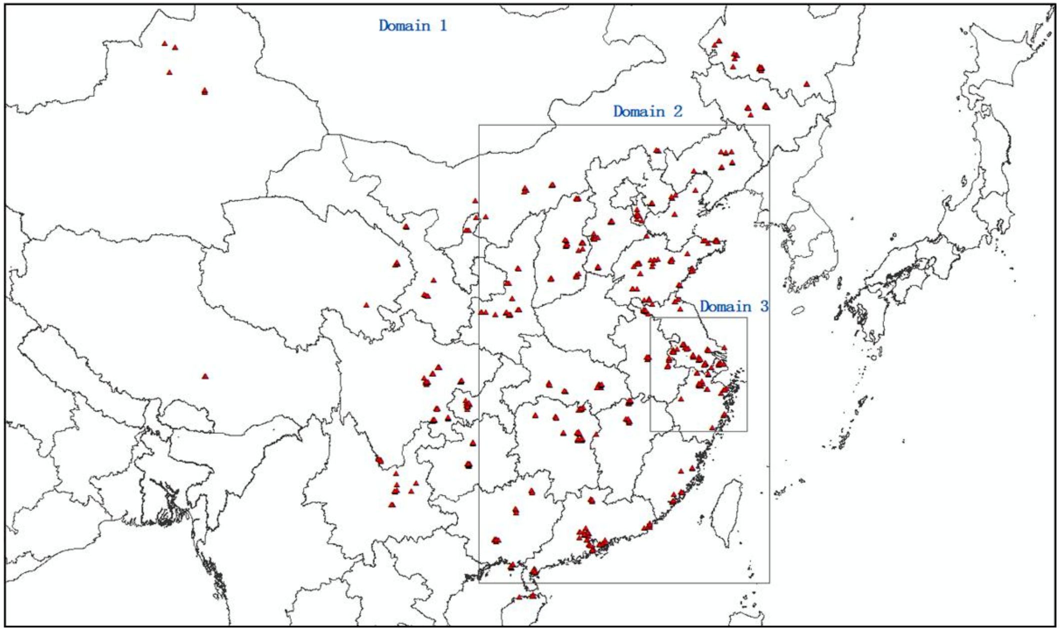

Fig. 1. Modeling domains and location of the monitoring sites used for model evaluation.

ACPD
13, 21507–21540, 2013

Sources and impacts of a dust event in the YRD

X. Fu et al.

Title Page
Abstract Introduction
Conclusions References
Tables Figures
◀◀ ▶▶
◀ ▶
Back Close
Full Screen / Esc
Printer-friendly Version
Interactive Discussion

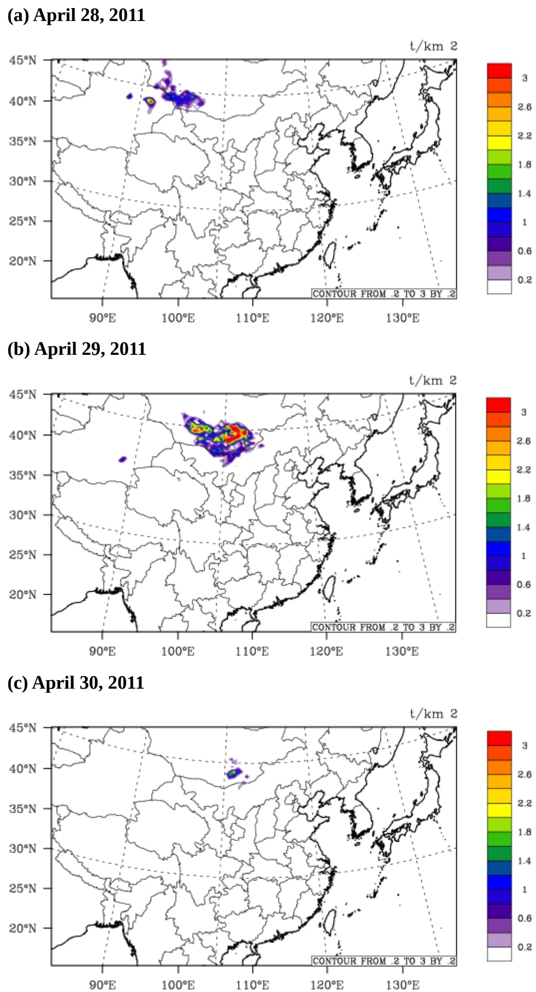

Fig. 2. The predicted daily mean dust PM_{10} emission on 28, 29 and 30 April.

Discussion Paper | Discussion Paper | Discussion Paper | Discussion Paper |

ACPD

13, 21507–21540, 2013

Sources and impacts of a dust event in the YRD

X. Fu et al.

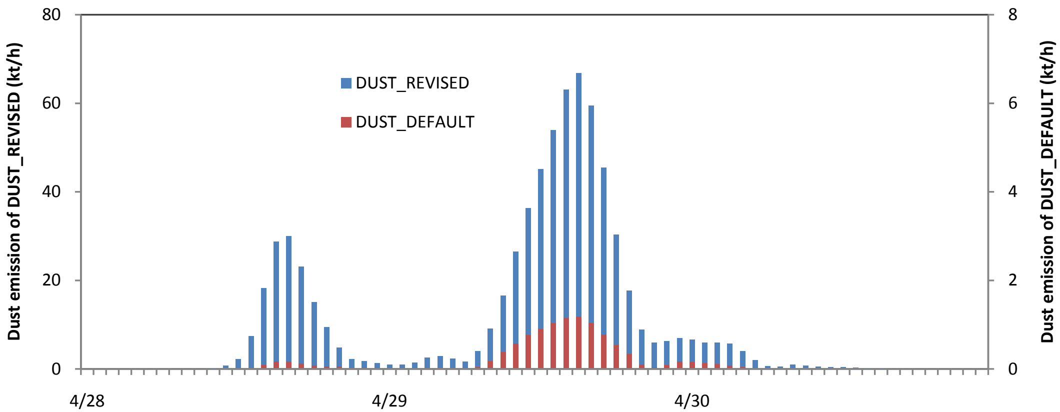

Fig. 3. The temporal variation of dust emissions.

ACPD
13, 21507–21540, 2013

Sources and impacts of a dust event in the YRD

X. Fu et al.

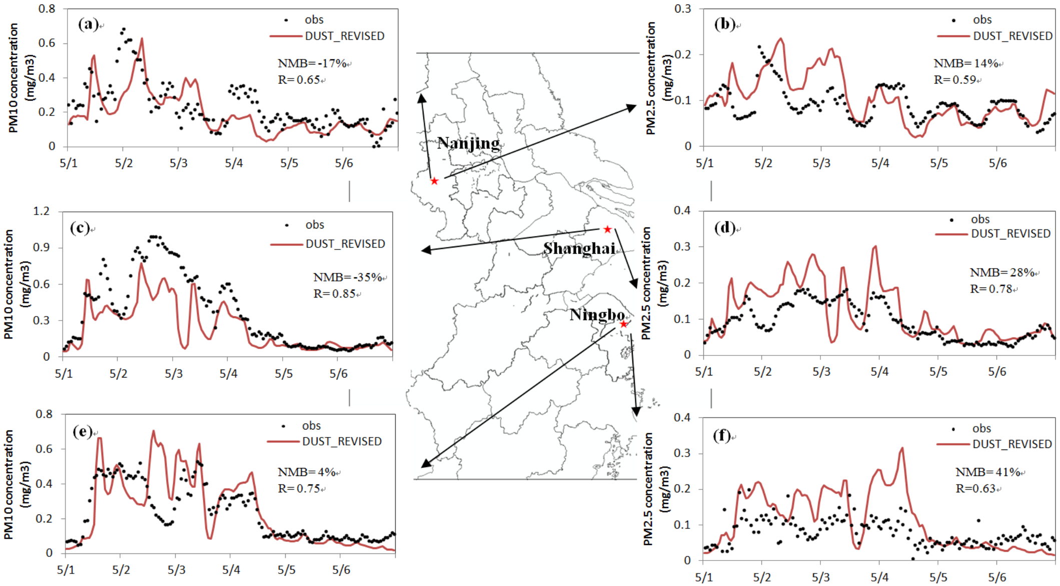

Fig. 4. Time series of hourly PM_{10} **(a, c, e)** concentration and $PM_{2.5}$ concentration **(b, d, f)** from observation and prediction with dust emission at three sites in the YRD region.

ACPD
13, 21507–21540, 2013

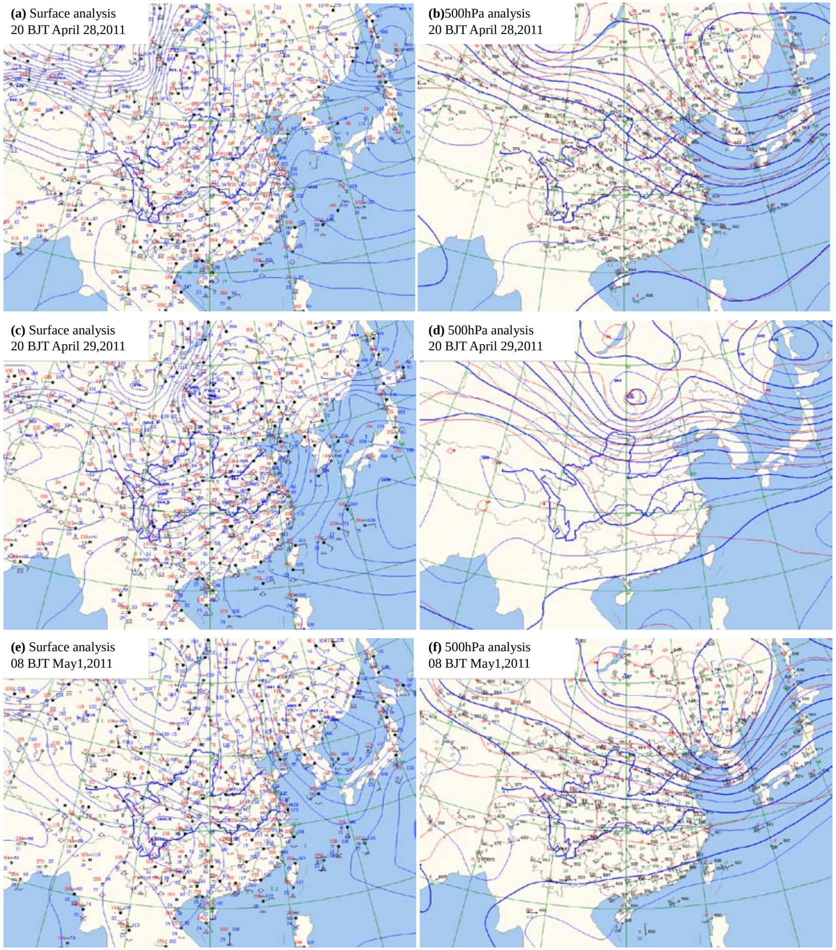

Fig. 5. Surface and 500 hPa weather chart in China.

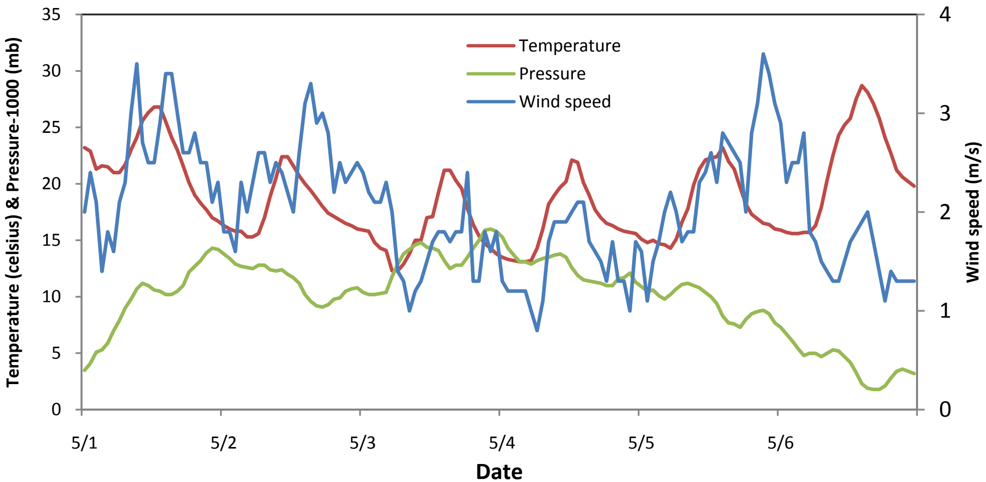

Fig. 6. Surface meteorological variables from 1 to 6 May in Shanghai monitoring site.

ACPD
13, 21507–21540, 2013

Sources and impacts of a dust event in the YRD

X. Fu et al.

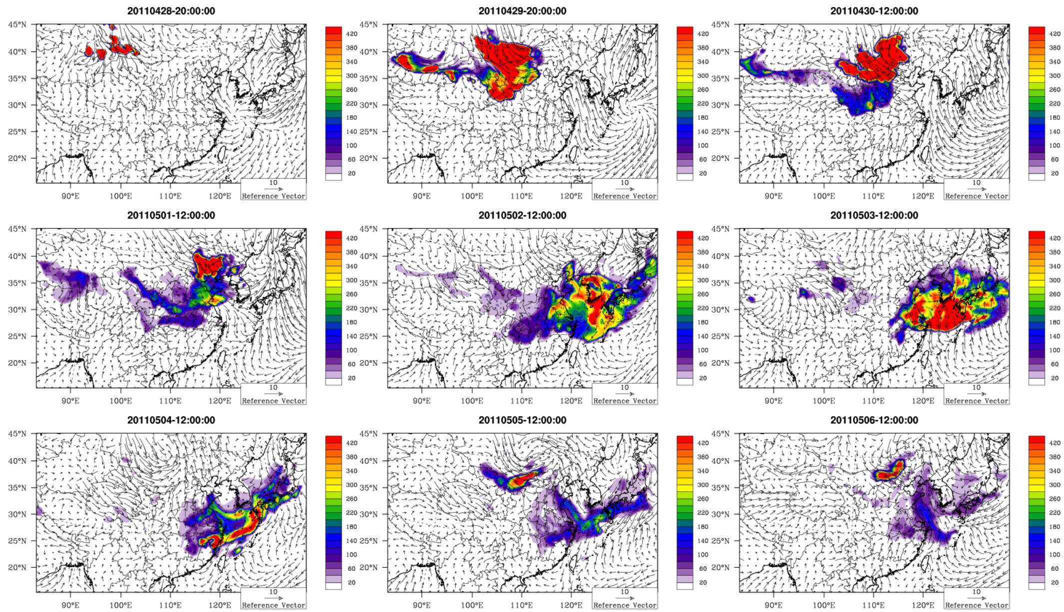

Fig. 7. The spatio-temporal variation of dust impacts on PM_{10} concentration ($\mu g\,m^{-3}$) during this dust event (DUST_REVISED minus DUST_OFF).

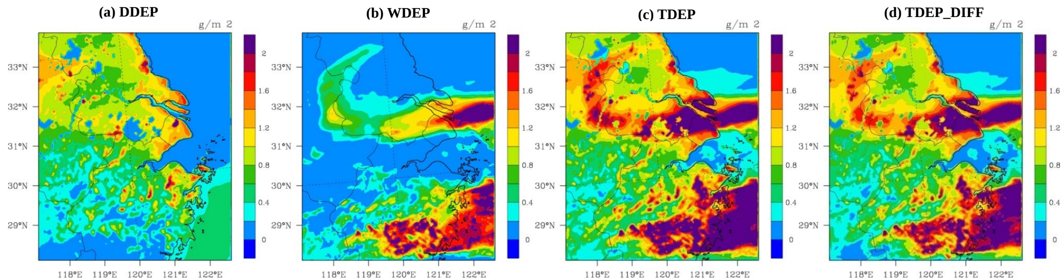

Fig. 8. PM_{10} deposition in the YRD region from 1 to 6 May.

ACPD
13, 21507–21540, 2013

Sources and impacts of a dust event in the YRD

X. Fu et al.

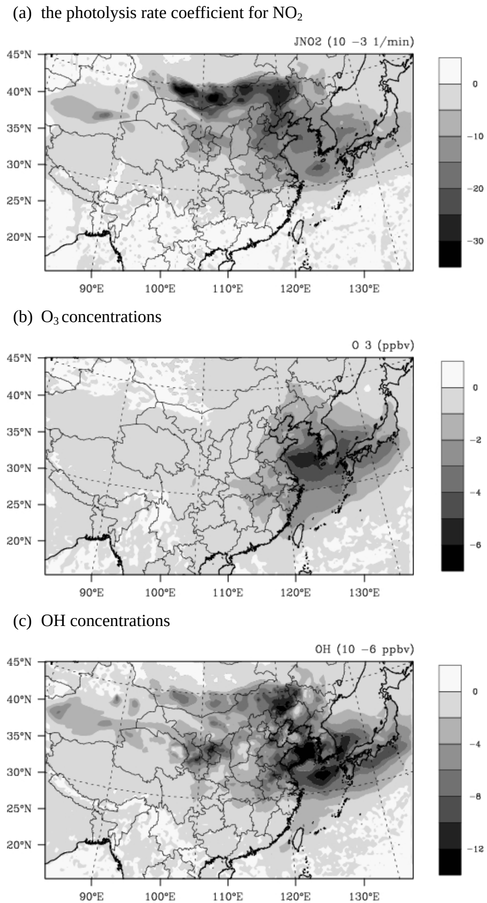

Fig. 9. Differences between simulations DUST_REVISED and DUST_OFF for the photolysis rate coefficient for NO_2 **(a)**, O_3 concentrations **(b)** and OH concentrations **(c)** averagely from 28 April to 6 May.

ACPD
13, 21507–21540, 2013

Sources and impacts of a dust event in the YRD

X. Fu et al.

Title Page
Abstract | Introduction
Conclusions | References
Tables | Figures
◀ | ▶
Back | Close
Full Screen / Esc
Printer-friendly Version
Interactive Discussion